Journal of AppliedMath, 2024, 2(5), 1797.
https://doi.org/10.59400/jam1797

Article

On mathematical analysis of the impact of bilinear therapeutic controls with monolytic vaccination for HBV infection model

Bassey Echeng Bassey

Department of Mathematics, University of Cross River State, Calabar 540252, Nigeria; echengba.rexson@yahoo.com

CITATION

Bassey BE. On mathematical analysis of the impact of bilinear therapeutic controls with monolytic vaccination for HBV infection model. Journal of AppliedMath. 2024; 2(5): 1797. https://doi.org/10.59400/jam1797

ARTICLE INFO

Received: 10 August 2024
Accepted: 26 September 2024
Available online: 15 October 2024

Abstract: While in acknowledgment of varying existing novel results on control of hepatitis B virus (HBV) dynamic infection, the methodological implementation of bilinear control functions in the presence of designated vaccination has not been explicitly considered. Therefore, the present investigation extending an existing study formulated and redeveloped a 6-dimensional HBV mathematical model that seeks and investigates the mathematical and epidemiological composition of the derived model as well as the methodological behavioral impact of applied bilinear therapeutic control functions and monolytic vaccination. The components of analytic predictions explored differential theory in conjunction with the classical Cauchy-Lipschitz condition. Numerical simulations were conducted using the in-built Runge-Kutta in a Mathcad surface. Results obtained indicated early decline of HBV viral load with intense rejuvenation of the recovered and susceptible state-space, following coherent induced bilinear control functions with designated vaccines. The study is highly recommended for HBV-related cases of co-infectivity.

Keywords: Cauchy-Lipchitz-condition; model-well-posedness; chronic-HBV-carrier; bilinear-control-function; monolytic-vaccination
MSC (2010): 93A30; 93C15; 34H15; 65L20

1. Introduction

Hepatitis B is arguably considered one of the deadliest diseases and has been created as a liver infection caused by the hepatitis B virus (HBV), which, under untreated scenarios, often leads to either liver cirrhosis, liver cancer, and hepatocellular carcinoma or, worse still, could aggravate to lethal consequences [1,2]. Biologically, HBV is considered a prototype member of the Hepadnaviride family (hepatotropic deoxynucleic acid-DNA virus), which constitutes hyper-string infection fibers to the liver cells and is traceable to the pancreas, kidney, and mononuclear cells [3,4]. In the study [5], the role of covalently closed circular deoxynucleic acid (cccDNA) in HBV maintenance was investigated and observed that though the molecular mechanisms responsible for HBV persistence seem not to be fully understood, the mechanism is multifactorial. Moreover, the unique replication of strategy deployed by HBV enhances its sustainability in infected hepatocytes. In a more precarious dimension, the observed stability of the HBV minichromosomal genome and the inability of the immune system to suppress chronic HBV infection substantiate a pivot mechanism for HBV chronicity [5]. Buttressing the aforementioned impact of cccDNA, the World Health Organization (WHO), in a key facts survey, revealed that an estimated 254 million people were living with chronic hepatitis B infection with 1.2 million new infections each year and a 1.1 million death toll [6].

Hepatitis B infection could assume a varying range from acute (short and severe) to chronic (long term) and has been a major cause of high mortality and morbidity rates worldwide [6]. Earlier investigations show that over 2 billion worldwide are infected with HBV, transmitting to 350 million chronic cases with an estimated 600,000 lethal consequences [3,7]. More complicated is the fact that the ubiquitous and asymptotic build-up of symptoms of HIV co-infectivity worsens early detection of HBV presence [8,9]. Perturbingly, HBV incubation period, which is known to be 30–180 days, seems not to be adequately understood, noting that several infectious cases are clinically documented after acute stages of the infection [10,11]. Unlike HIV, risk factors accompanying chronic HBV include its progression to HBsAg, anti-HBeAg, and HBV-DNA, as well as problems of HAART toxicity, as often is the case for co-infection. HBV transmission mode cut across percutaneous (horizontal) or direct contact with infected body fluids like blood, silver, vaginal fluids, and semen, as well as perinatal or vertical transmission, i.e., mother-to-child [6,12]. For chronic monolithic HBV, literature has revealed that possible chemotherapies include application of interferon in the form of standard or PEGylated IFN, which is the nucleos(t)ide analogues (NAs), among others [1,13,14]. Of note, early management of HBV infection could lead to permanent recovery due to intense build-up of the immune system [15].

Interestingly, the dynamics of HBV transmission, treatment, and control measures are studied and understood using classical mathematical modeling among other methods. That is, several novel mathematical models have been formulated in this direction. For instance [16], a mathematical model had been formulated that studied the characteristics of HV = BV transmission dynamics. That investigation explored the fundamental theory of differential equations. Results obtained gave explicit impact of long-term exposure to a population with acute and chronic HBV [17], extending the above model by formulating a 5-dimensional HBV epidemiological model with a linear control function but could not distinguish recovery compartments and was devoid of a vaccinated subpopulation. Further investigation was conducted by extending the latter model with the incorporation and redefinition of three compartments—latent, carriers, and recovery in the presence of monolithic vaccination [1]. That is, the model explored a 6-dimensional mathematical dynamic but without any clear-cut indications of some paramount indicators in the form of treatment rate and impact of proliferated recovered subpopulation. Moreover, the nature of the vaccine was not specified.

Other studies [18,19] demonstrated the fact that acute HBV infection could be found in newborns of infected mothers. In related co-infectivity, [12] formulated a 7-dimensional HIV-HBV mathematical model that investigated the interplay of these subpopulations with multi-therapies in the presence of a dual-adaptive immune system and intracellular delay function. The exclusion of both latent cells and non-cytotoxic carriers was adopted, noting that identification of these stages often occurs at the acute stage of the infection transmission, an approach conducted by [20]. On the premise of these seeming incoherent literatures for HBV, the present study is primed by the investigation of the impact of the application of the bilinear control function induced by designated linear vaccination. Therefore, adopting the innovative ideas of [12] and extending existing model [1], the objectives of the study are to seek and formulate a

6-dimensional homogenous dynamic mathematical model investigated using bilinear control functions in the presence of monolithic vaccination. Moreover, the novelty of the investigation is in the determination of distinct specifications of both the directional impact of the recovered compartment on the susceptible and the rate of induced treatment control functions with enhanced vaccination on infectious subpopulations.

Therefore, the composition of this present investigation revolves around 6 sections, with Section 2, devoted to the materials and methods as adopted in this work. Section 3 focuses on the analytical prediction of system well-posedness. The computational illustrations arising from analytical predictions are domiciled in Section 4. Resultant analysis in the form of discussion forms the fulcrum of Section 5. Finally, we devote Section 6 to the invaluable remarks and conclusion of the study. Remarkably, this investigation is targeted to exhume insight into the methodological application of bilinear control functions in the presence of monolithic vaccination with the intense possibility of eradicating this deadly virus—HBV.

2. Materials and methods

The materials and methods adopted in this investigation are thematically determined by the problem statement of the study and model derivation. Basically, using ordinary differential equations, we investigate a 6-dimensional HBV mathematical model via the interplay of bilinear control functions (anti-hepatitis B surface/encore antigens–HBs e Ag and alanine amino-transferase–ALT) in the presence of a monolithic vaccine (Recombivax–Merck) at one dose of 40 meg/mL, on a three-dose of 0, 1, and 6 months [21]. The investigation of system analytical predictions explored the differential method in conjunction with the concept of the Cauchy-Lipschitz condition. Numerical computations exclusively deployed in-built Runge-Kutta of order of precision 4 in a Mathcad surface.

2.1. Problem statement of the study

Remarkably, the use of mathematical modeling in studying HBV transmission, control, and prevention dynamics has been severely conducted. However, accounting for model well-posedness using the Cauchy-Lipschitz condition and incisive application of both designated treatment functions and vaccination with enhanced parameter values has not been given the desired consideration. For instance, the model [12] had investigated the application of multi-therapies with dual-immune response for the treatment of dual-delayed HIV-HBV co-infectivity using optimal control strategy. Of interest, with the novel results attained from this study, the investigation couldn’t account for the analytical deployment of the Cauchy-Lipschitz condition in its mathematical analysis coupled with the non-inclusion of the vaccinated compartment. More so, [1] had considered the HBV model with the incorporation of a vaccine-treated chamber but without accounting for the system's well-posedness and the consequential impact of the recovered population on the system, as well as non-numeric value for control parameters.

Therefore, in this present investigation, extending the latter model, the investigation seeks to account for the reunification of the proliferated recovered

population and the thematic determination of system model well-posedness, as well as quantify immunization enhancement parameters in the presence of designated vaccination.

2.2. Derivation of model mathematical equations

The present investigation is initialized by giving a brief outline of the system motivating model [1]. The aforementioned model was developed using 6 subpopulations with the primary aim of investigating the impact of vaccination on an HBV dynamics model (readers are encouraged to access the paper for more details). Of note, the biological derivation of the model was given as:

$$\begin{cases} \frac{dX}{dt} = \mu\omega(1\text{-vC}) - \lambda X - \sigma X + (1-\sigma)Y - \mu_1 X \\ \frac{dY}{dt} = \mu(1-\omega) + \sigma X - (1-\sigma)Y - \mu_1 Y \\ \frac{dL}{dt} = \mu\omega vC + \xi\lambda X - \omega_1\varepsilon_1 L - \beta_1\varepsilon_2 L - \omega_2\psi_e\lambda L - \mu_1 L \\ \frac{dI}{dt} = (1-\xi)\lambda X + \omega_1\varepsilon_1 L + \omega_2\psi_e\lambda L + \omega_3\psi_c\lambda C - \beta_2\varepsilon_3 I - \beta_3 t_1 I - \mu_1 I - \mu_2 I \\ \frac{dC}{dt} = \beta_1\varepsilon_2 L + \beta_2\varepsilon_2 \text{I} - \omega_3\psi_c\lambda \text{C} - \beta_4 t_1 C - \mu_1 C - \mu_2 C + \omega_4\psi_r\lambda R \\ \frac{dR}{dt} = \beta_3 t_1 I + \beta_4 t_1 C \text{ - } \omega_4\psi_r\lambda \text{R - } \mu_1 R \end{cases} \quad (1)$$

where $\{(X,Y,L,I,C,R) \in N(t)\} \geq 0$ for all $t_0 \in t = 0$, are the model state-space having initial time t_0. For detail description of both model state-space and parameters, we refer readers to the aforementioned authors.

Thus, in extending and restructuring this model, the present investigation seeks to incorporate the following:

1) Reunification of proliferated recovered population with the susceptible compartment.
2) Redefined with appropriate valuation of rate of immunization of latently infected and chronic HBV population.
3) Analytical deployment of classical Cauchy-Lipchitz condition in evaluation of model well-posedness.
4) Detection and valuation of unprotected chronic carriers.
5) Specification of vaccination control function.
6) Conduction of numerical computation using in-built Runge-Kutter of order of precision 4 in a Mathcad surface.

More significant in model building is the conceptualization of model assumptions. Therefore, the present model in conjunction with existing assumptions [1,12], the following assumptions holds:

Assumptions

1) Redefinition of existing model to capture reunification of proliferated recovered population, i.e. $rR(t) \rightarrow X_p(t)$.
2) Immunization could take place on day-one of child birthing, i.e. $(1-\sigma) > 0$ for all $0 \leq \sigma \leq 1$.
3) Chronic carriers subpopulation are vaccinated arte the rate $\sigma \geq 0$.

4) Only acute infectious and chronic carriers die due to infection, i.e. $\mu_2 \geq 0$.
5) Unprotected chronic carriers are detected at rate $v \geq 0$.
6) Natural exists in all compartments i.e. $\mu_1 \geq 0$.
7) Only the acute infectious and chronic carriers transmit the virus i.e. $\beta \geq 0$.

On a general assumption is the fact that if we let $N(t)$ denote the total homogeneously mixing population understudy at time $t \in [t_0, t_f]$, then this host population is partitioned into six subpopulations: the susceptible individuals $X_p(t)$, the protective immunized subpopulation $Y(t)$ and the latently infected individuals $L(t)$. Others include acute infected class $I(t)$, the chronic HBV carriers $C(t)$ and the recovered subpopulation that reunite with the susceptible denoted by $R(t)$. This, accounting for this homogeneous subpopulations and assumptions, the present epidemiological equation of the system is derived as follows:

$$\begin{cases} \dot{X_p}(t) = b_p\omega(1-\mathrm{vC}) + (1-\sigma)Y + rR - \lambda X_p - (\sigma+\mu_1)X_p \\ \dot{Y}(t) = b_p(1-\omega) + \sigma X_p - (1-\sigma)Y - \mu_1 Y \\ \dot{L}(t) = b_p\omega vC + \xi\lambda X_p - \omega_1\varepsilon_1 L - \beta_1\varepsilon_2 L - \omega_2\psi_e\lambda L - \mu_1 L \\ \dot{I}(t) = (1-\xi)\lambda X_p + \omega_1\varepsilon_1 L + \omega_2\psi_e\lambda L + \omega_3\psi_c\lambda C - \beta_2\varepsilon_3 I - \beta_3 t_1 I - (\mu_1+\mu_2 \\ \dot{C}(t) = \beta_1\varepsilon_2 L + \beta_2\varepsilon_2 \mathrm{I} - \omega_3\psi_c\lambda \mathrm{C} - \beta_4 t_1 C + \omega_4\psi_r\lambda R - (\mu_1+\mu_2)C \\ \dot{R}(t) = \beta_3 t_1 I + \beta_4 t_1 C - \omega_4\psi_r\lambda \mathrm{R} - (\mu_1+r)R \end{cases} \quad (2)$$

where $\{(X_p, Y, L, I, C, R) \in N(t)\} \geq 0$ for all $t_0 \in t = 0$, are the model state-space having initial time t_0. That is, the total population understudy id given by

$$(t) = X_p(t) + Y(t) + L(t) + I(t) + C(t) + (t)R = 1 \quad (3)$$

and having system force of infection defined by

$$\lambda = \beta\frac{(I+\eta C)}{N(t)} \quad (4)$$

Equations (2)–(4) is schematically represented by **Figure 1**:

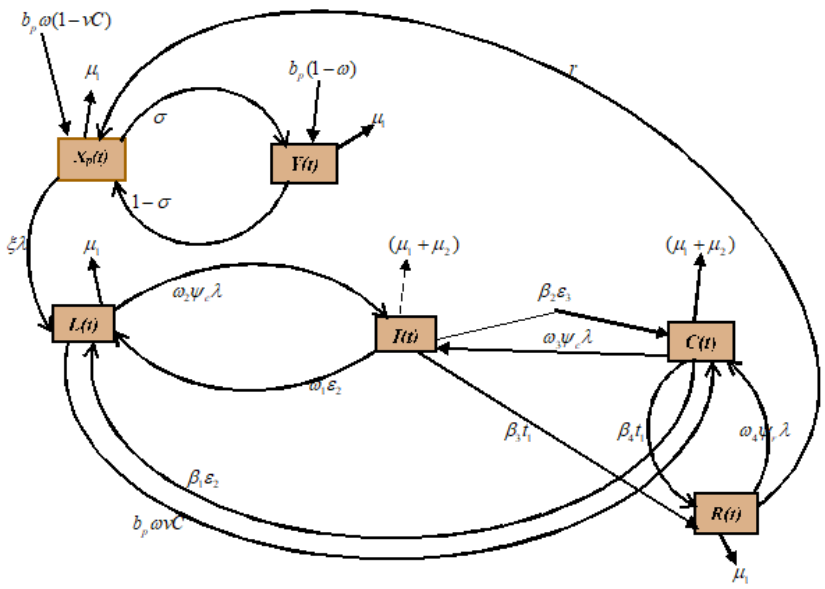

Figure 1. An epidemiological flow chart for the transmission dynamics of HBV infection.

Intuitively, we represent the biological description of both state-space and parameter variables of model (2) and **Figure 1** as depicted by **Tables 1** and **2**:

Table 1. Description of state space for model (2).

Symbols	Description
X_p	Susceptible population
Y	Protective Immunized population
L	Latently infected population
I	Acute infectious population
C	Chronic carriers population
R	Treated recovered population

Table 2. Description of model parameter variables.

Symbols	Description
X_p	Natural birth rate
ω	Proportion of birth rate without protective immunity
$(1-\omega)$	Proportion of birthrate with protective immunity
σ	Vaccination rate
$(1-\sigma)$	Unsuccessful vaccination rate
μ_1	Natural death rate
μ_2	Death rate due to infection
λ	Force of infection
β	Effective contact rate for HBV infection
η	Rate of infectiousness of carriers relative to acute infection
ε_1	Transfer rate from latent to acute
ε_2	Transfer rate from latent to carrier
ε_3	Transfer rate from acute to carrier
β_1	Transmission probability from latent to carrier
β_2	Transmission probability from acute to carrier
β_3	Transmission probability from acute to recovered acquiring treatment
β_4	Transmission probability from carriers to recovered acquiring treatment
t_1	Rate of treatment
$(1-\xi)$	The fraction of the newly individuals who are fast progresses
ψ_e	Reinfection rate of latent individuals
v	Rate at which carrier mothers are immunized
ω_1	Fraction of latent individuals who develop symptoms are infected
ω_2	Fraction of re-infected latent individuals who are infected
ω_3	Fraction of re-infected carrier individuals who are infected
ω_4	Fraction of recovered individuals who are infected
r	Recovered reuniting with the susceptible

Next, we are confronted with the determination of model analytical predictions.

3. Analysis of model mathematical properties

In diffusing the model mathematical properties, we are required to thematically account for the system positivity of the solution, the system boundedness of the solution, and the existence of the system solution.

3.1. Positivity of system solution

In this sub-section, we attempt to show that all state space, which are exact representation of set of living organisms are all positive for all $t \geq 0$. That is, we present analytic computation of the model positivity using the following theorem.

Theorem 1. *(Positivity) Let the system initial conditions be given by* $\{X_p(0), Y(0), L(0), I(0), C(0), R(0)\} \in \Re_+^6$. Then, the solution set $\{X_p(t), Y(t), L(t), I(t), C(t), R(t)\}$ *for system (2) remains positive for all* $t \geq 0$.

Proof. Here, we apply existing studies [22,23]. In this case, taking on the first equation of system (1), we have.

$$\dot{X_p}(t) = b_p\omega(1\text{-vC}) + (1-\sigma)Y + rR - \lambda X_p - (\sigma + \mu_1)X_p$$

Taking the differential of X_p with respect to time t, we have

$$\dot{X_p}(t) = b_p\omega - (\sigma + \lambda + \mu_1)X_p$$

Then, by separation of variables, we have

$$\dot{X_p}(t) + (\sigma + \lambda + \mu_1)X_p = b_p\omega$$

The solution of the equation is obtained by applying the integrating factor method $IF = e^{\int(\sigma+\lambda+\mu_1)dt} = e^{(\sigma+\lambda+\mu_1)t}$. That is, by multiplying both side of the above by the integrating factor *IF*, we have

$$e^{(\sigma+\lambda+\mu_1)t}\dot{X_p}(t) + (\sigma + \lambda + \mu_1)X_p e^{(\sigma+\lambda+\mu_1)t} = b_p\omega e^{(\sigma+\lambda+\mu_1)t}$$

or

$$\frac{d}{dt}[(\sigma + \lambda + \mu_1)]X_p e^{(\sigma+\lambda+\mu_1)t} = b_p\omega e^{(\sigma+\lambda+\mu_1)t}$$

Integrating, we have

$$X_p e^{(\sigma+\lambda+\mu_1)t} = \frac{b_p\omega}{(\sigma + \lambda + \mu_1)} e^{(\sigma+\lambda+\mu_1)t} + K$$

Where K is the constant of integration, simplifying we have

$$X_p(t) = \frac{b_p\omega}{(\sigma + \lambda + \mu_1)} + K\, e^{-(\sigma+\lambda+\mu_1)t} \tag{5}$$

Applying the initial condition i.e. $t = 0 \Rightarrow X_p(t) = X_p(0)$. Then, Equation (5) becomes

$$X_p(0) = \frac{b_p\omega}{(\sigma + \lambda + \mu_1)} + K$$

or

$$X_p(0) - \frac{b_p\omega}{(\sigma+\lambda+\mu_1)} = K$$

Substituting K into Equation (5) we obtain

$$X_p(t) = \frac{b_p\omega}{(\sigma+\lambda+\mu_1)} + \left[X_p(0) - \frac{b_p\omega}{(\sigma+\lambda+\mu_1)}\right] e^{-(\sigma+\lambda+\mu_1)t} \geq 0.$$

Hence, since $(\sigma+\lambda+\mu_1) > 0$ then, $X_p(0) > 0$ as $t = 0$ and $X_p(t) \leq 0$ as $t \to \infty$.

From the immunized individuals $Y(t)$, we have

$$\dot{Y}(t) = b_p(1-\omega) + \sigma X_p - (1-\sigma)Y - \mu_1 Y$$

Taking the differentiation of Y with respect to time t, we have

$$\dot{Y}(t) = b_p(1-\omega) - [(1-\sigma)+\mu_1]Y$$

Then, by separation of variables, we have

$$\dot{Y}(t) + [(1-\sigma)+\mu_1]Y = b_n(1-\omega)$$

The solution of the equation is obtained by using the integrating factor method, $IF = e^{\int[(1-\sigma)+\mu_1]dt} = e^{[(1-\sigma)+\mu_1]t}$. That is, by multiplying both side of the above by the integrating factor *IF*, we have

$$e^{[(1-\sigma)+\mu_1]t}Y'(t) + [(1-\sigma)+\mu_1]Ye^{[(1-\sigma)+\mu_1]t} = b_n(1-\omega)e^{[(1-\sigma)+\mu_1]t}$$

or

$$\frac{d}{dt}[(1-\sigma)+\mu_1]Ye^{[(1-\sigma)+\mu_1]t} = b_n(1-\omega)e^{[(1-\sigma)+\mu_1]t}$$

Integrating, we have

$$\mathrm{Y}e^{[(1-\sigma)+\mu_1]t} = \frac{b_n(1-\omega)}{[(1-\sigma)+\mu_1]}e^{[(1-\sigma)+\mu_1]t} + K$$

where K is the constant of integration. Simplifying, we have

$$Y(t) = \frac{b_p(1-\omega)}{[(1-\sigma)+\mu_1]} + Ke^{-[(1-\sigma)+\mu_1]t} \tag{6}$$

Applying the initial condition i.e. as$t = 0 \Rightarrow \mathrm{Y}(t)$=Y(0). Then, Equation (6) becomes

$$\mathrm{Y}(0) = \frac{b_p(1-\omega)}{[(1-\sigma)+\mu_1]} + K$$

or

$$\mathrm{Y}(0) - \frac{b_p(1-\omega)}{[(1-\sigma)+\mu_1]} = K$$

Substituting K into Equation (6) we obtain

$$\mathrm{Y}(t) = \frac{b_p(1-\omega)}{[(1-\sigma)+\mu_1]} + \left\{Y(0) - \frac{b_p(1-\omega)}{[(1-\sigma)+\mu_1]}\right\} e^{-[(1-\sigma)+\mu_1]t} \geq 0$$

Hence, since $[(1-\sigma)+\mu_1] > 0$ then, $Y(0) > 0$ as $t = 0$ and $Y(t) \leq 0$ as $t = 0$ and thus, $Y(t) \leq 1$ as $t \to \infty$.

From the latent individuals, $L(t)$ we have

$$\dot{L(t)} = b_p\omega v C + \xi\lambda X_p - \omega_1\varepsilon_1 L - \beta_1\varepsilon_2 L - \omega_2\psi_e\lambda L - \mu_1 L.$$

Taking the differential of L with respect to time t, we have

$$\dot{L(t)} = -(\omega_1\varepsilon_1 + \beta_1\varepsilon_2 + \omega_2\psi_e\lambda + \mu_1)L$$

or

$$\dot{L(t)} + (\omega_1\varepsilon_1 + \beta_1\varepsilon_2 + \omega_2\psi_e\lambda + \mu_1)L = 0$$

The solution of the equation is obtained by using the integrating factor method, $IF = e^{\int[\omega_1\varepsilon_1+\beta_1\varepsilon_2+\omega_2\psi_e\lambda+\mu_1]dt} = e^{(\omega_1\varepsilon_1+\beta_1\varepsilon_2+\omega_2\psi_e\lambda+\mu_1)t}$. That is, by multiplying both side of the above by the integrating factor *IF*, we have

$$e^{(\omega_1\varepsilon_1+\beta_1\varepsilon_2+\omega_2\psi_e\lambda+\mu_1)t}\dot{L(t)} + (\omega_1\varepsilon_1 + \beta_1\varepsilon_2 + \omega_2\psi_e\lambda + \mu_1)Le^{(\omega_1\varepsilon_1+\beta_1\varepsilon_2+\omega_2\psi_e\lambda+\mu_1)t} = 0$$

or

$$\frac{d}{dt}[(\omega_1\varepsilon_1 + \beta_1\varepsilon_2 + \omega_2\psi_e\lambda + \mu_1)]Le^{(\omega_1\varepsilon_1+\beta_1\varepsilon_2+\omega_2\psi_e\lambda+\mu_1)t} = 0$$

Integrating, we have

$$\mathrm{L}e^{(\omega_1\varepsilon_1+\beta_1\varepsilon_2+\omega_2\psi_e\lambda+\mu_1)t} = K$$

where K is the constant of integration. Simplifying we have

$$L(t) = Ke^{-(\omega_1\varepsilon_1+\beta_1\varepsilon_2+\omega_2\psi_e\lambda+\mu_1)t} \quad (7)$$

Applying the initial condition i.e. $t = 0 \Rightarrow L(t) = L(0)$. Then, the above equation becomes

$$\mathrm{L}(0) = K$$

Substituting K into Equation (7) we obtain

$$\mathrm{L}(t) = \mathrm{L}(0)e^{-(\omega_1\varepsilon_1+\beta_1\varepsilon_2+\omega_2\psi_e\lambda+\mu_1)t} \geq 0$$

Hence, since $[(\omega_1\varepsilon_1 + \beta_1\varepsilon_2 + \omega_2\psi_e\lambda + \mu_1)] > 0$ then, $L(0) > 0$ as $t = 0$ and $L(t) \leq 0$ as $t \to \infty$.

From acute individuals $I(t)$, we have

$$\dot{I(t)} = (1-\xi)\lambda X_p + \omega_1\varepsilon_1 L + \omega_2\psi_e\lambda L + \omega_3\psi_c\lambda C - \beta_2\varepsilon_3 I - \beta_3 t_1 I - (\mu_1+\mu_2)I$$

Taking the differential of I with respect to t, we have

$$\dot{I(t)} = -(\beta_2\varepsilon_3 + \beta_3 t_1 + \mu_1 + \mu_2)I$$

or

$$\dot{I}(t) + (\beta_2\varepsilon_3 + \beta_3 t_1 + \mu_1 + \mu_2)I = 0$$

The solution of the equation is obtained by using the integrating factor i.e. $IF = e^{\int[\beta_2\varepsilon_3+\beta_3 t_1+\mu_1+\mu_2]dt} = e^{(\beta_2\varepsilon_3+\beta_3 t_1+\mu_1+\mu_2)t}$. That is, by multiplying both side of the above by the integrating factor *IF*, we have

$$e^{(\beta_2\varepsilon_3+\beta_3 t_1+\mu_1+\mu_2)t} I'(t) + (\beta_2\varepsilon_3 + \beta_3 t_1 + \mu_1 + \mu_2) I e^{(\beta_2\varepsilon_3+\beta_3 t_1+\mu_1+\mu_2)t} = 0$$

Integrating, we have

$$\mathrm{I}e^{(\beta_2\varepsilon_3+\beta_3 t_1+\mu_1+\mu_2)t} = K$$

where *K* is the is the constant of integration, simplifying we have

$$I(t) = Ke^{-(\beta_2\varepsilon_3+\beta_3 t_1+\mu_1+\mu_2)t} \tag{8}$$

Applying the initial condition i.e. $t = 0 \Rightarrow I(t) = I(0)$.Then Then Equation (8) becomes

$$\mathrm{I}(0) = K$$

Substituting *K* into Equation (8) we obtain

$$\mathrm{I}(t) = I(0)e^{-(\beta_2\varepsilon_3+\beta_3 t_1+\mu_1+\mu_2)t} \geq 0$$

Hence, since $(\beta_2\varepsilon_3 + \beta_3 t_1 + \mu_1 + \mu_2) > 0$ then, $I(0) > 0$ as $t = 0$ and $I(t) \leq 0$ as $t \to \infty$.

From the chronic individuals $C(t)$, we have

$$\dot{C}(t) = \beta_1\varepsilon_2 L + \beta_2\varepsilon_2 \mathrm{I} - \omega_3\psi_c\lambda \mathrm{C} - \beta_4 t_1 C + \omega_4\psi_r\lambda R - (\mu_1 + \mu_2)C$$

Taking the differential of $C(t)$ with respect to t, we have

$$\dot{C}(t) = -(\omega_3\psi_c\lambda + \beta_4 t_1 + \mu_1 + \mu_2)C$$

or

$$\dot{C}(t) + (\omega_3\psi_c\lambda + \beta_4 t_1 + \mu_1 + \mu_2)C = 0$$

The solution of the equation is obtained by using the integrating factor i.e.

$IF = e^{\int[(\omega_3\psi_c\lambda+\beta_4 t_1+\mu_1+\mu_2)]dt} = e^{(\omega_3\psi_c\lambda+\beta_4 t_1+\mu_1+\mu_2)t}$. That is, by multiplying both side of the above by the integrating factor *IF*, we have

$$e^{(\omega_3\psi_c\lambda+\beta_4 t_1+\mu_1+\mu_2)t} C'(t) + (\omega_3\psi_c\lambda + \beta_4 t_1 + \mu_1 + \mu_2) C e^{(\omega_3\psi_c\lambda+\beta_4 t_1+\mu_1+\mu_2)t} = 0$$

or

$$\frac{d}{dt}[(\omega_3\psi_c\lambda + \beta_4 t_1 + \mu_1 + \mu_2)] C e^{(\omega_3\psi_c\lambda+\beta_4 t_1+\mu_1+\mu_2)t} = 0$$

Integrating, we have

$$\mathrm{C}e^{(\omega_3\psi_c\lambda+\beta_4 t_1+\mu_1+\mu_2)t} = K$$

where *K* is the is the constant of integration, simplifying we have:

$$C(t) = Ke^{-(\omega_3\psi_c\lambda+\beta_4 t_1+\mu_1+\mu_2)t} \tag{9}$$

Applying the initial condition i.e. $t = 0 \Rightarrow C(t) = C(0)$. Then, Equation (9) becomes

$$\mathrm{C}(0) = K$$

Substituting K into Equation (9) we obtain

$$\mathrm{C}(t) = C(0)e^{-(\omega_3\psi_c\lambda+\beta_4 t_1+\mu_1+\mu_2)t} \geq 0$$

Hence, since $[(\omega_3\psi_c\lambda + \beta_4 t_1 + \mu_1 + \mu_2)] > 0$ then, $C(0) > 0$ as $t = 0$ and $C(t) \leq 0$ as $t \to \infty$.

From the recovered individuals $R(t)$, we have

$$\dot{R}(t) = \beta_3 t_1 I + \beta_4 t_1 C - \omega_4\psi_r\lambda R - (r + \mu_1)R$$

Taking the differential of R with respect to t, we have

$$\dot{R}(t) = -(\omega_4\psi_r\lambda + r + \mu_1)R$$

or

$$\dot{R}(t) + (\omega_4\psi_r\lambda + r + \mu_1)R = 0$$

The solution of the equation is obtained by using the integrating factor i.e. $IF = e^{\int[\omega_4\psi_r\lambda + \mu_1+r]dt} = e^{(\omega_4\psi_r\lambda+\mu_1+\mathrm{r})t}$. That is, by multiplying both side of the above by the integrating factor *IF*, we have

$$e^{(\omega_4\psi_r\lambda + \mu_1)t}R'(t) + (\omega_4\psi_r\lambda + \mu_1+\mathrm{r})Re^{(\omega_4\psi_r\lambda + \mu_1)t} = 0$$

Integrating, we have

$$\mathrm{R}e^{(\omega_4\psi_r\lambda + \mu_1+\mathrm{r})t} = K$$

where K is the is the constant of integration, simplifying we have

$$R(t) = Ke^{-(\omega_4\psi_r\lambda + \mu_1)t} \tag{10}$$

Applying the initial condition i.e. $t = 0 \Rightarrow R(t) = R(0)$. Then, Equation (10) becomes

$$\mathrm{R}(0) = K$$

Substituting K into Equation (7) we obtain

$$\mathrm{R}(t) = R\,(0)e^{-(\omega_4\psi_r\lambda + \mu_1)t} \geq 0$$

Hence, since $[(\omega_4\psi_r\lambda + \mu_1+\mathrm{r})] > 0$, then, $R(0) > 0$ as $t = 0$ and $R(t) \leq 0$ as $t \to \infty$.

Therefore, any solution of system (2) is such that the set: $\{(X_p(0), Y(0), L(0), I(0), C(0), R(0)) \geq 0\} \in \Re_+^6$ and the proof is completed. □

3.2. Boundedness of system solution

Here, we initiate the investigation for the system boundedness by first showing that the differential sum of the model equations is completely a function of system natural birth rate and natural clearance rate as well as death due to infection.

It is obvious that the system differential sum from Equation (2) is given by

$$\frac{dN}{dt}=\frac{dX_p}{dt}+\frac{dY}{dt}+\frac{dL}{dt}+\frac{dI}{dt}+\frac{dC}{dt}+\frac{dR}{dt}=b_p\omega(1-vC)-\lambda X_p+rR+(1-\sigma)Y-(\sigma+r+\mu_1)X_p+b_p(1-\omega)$$
$$+\sigma X_p-(1-\sigma)Y-\mu_1 Y+b_n\omega vC+\xi\lambda X_p-\omega_1\varepsilon_1 L-\beta_1\varepsilon_2 L$$
$$-\omega_2\psi_e\lambda L-\mu_1 L+(1-\xi)\lambda+\omega_1\varepsilon_1 L+\omega_2\psi_e\lambda L+\omega_3\psi_c\lambda C$$
$$-\beta_2\varepsilon_3 I-\beta_3 t_1 I-\mu_1 I-\mu_2 I+\beta_1\varepsilon_2 L+\beta_2\varepsilon_3 I-\omega_3\psi_c\lambda C$$
$$-\beta_4 t_1 C-\mu_1 C-\mu_2 C+\omega_4\psi_r\lambda R+\beta_3 t_1 I+\beta_4 t_1 C-\omega_4\psi_r\lambda R-(r+\mu_1)R$$

Simplifying, we obtain,

$$\begin{aligned}\frac{dN}{dt}&=b_p-\mu_1 X_p-\mu_1 Y-\mu_1 L-\mu_1 I-\mu_1 C-\mu_1 R-\mu_2 I-\mu_2 C\\&=b_p-\mu_1 N-\mu_2 I-\mu_2 C\end{aligned}\tag{11}$$

since $N(t)=\left\{X_p(t)+Y(t)+L(t)+I(t)+C(t)+R(t)\right\}=1$.

The following theorem satisfies the boundedness of system solution.

Theorem 2. *(Boundedness). Suppose system (2) is bounded in a closed set* $\Re_D=\left\{(X_p,Y,L,I,C,R)\in\Re_+^6:N\leq\frac{b_p}{\mu_1}\right\}$.

Then, all the solution of the closed set $\Re_D$ *is bounded, positively invariant and attracting with respect to system (2).*

Proof. Adopting classical approach for boundedness as applied by [24,25]. We recall Equation (11) i.e.

$$\frac{dN}{dt}=b_n-\mu_1 N-\mu_2 I-\mu_2 C$$

or

$$\frac{dN}{dt}+\mu_1 N=b_n-\mu_2 I-\mu_2 C$$

At zero mortality rate μ_2=0 then we have,

$$\frac{dN}{dt}+\mu_1 N=b_p$$

The solution of the equation is obtained by applying the integrating factor, $IF=e^{\int\mu_1 dt}=e^{\mu_1 t}$

$$e^{\mu_1 t}\frac{dN}{dt}+\mu_1 N e^{\mu_1 t}=b_p e^{\mu_1 t}$$

Integrating we have,

$$e^{\mu_1 t}N=\frac{b_p}{\mu_1}e^{\mu_1 t}+K$$

where K is the constant of integration, simplifying we obtain

$$N(t)=\frac{b_p}{\mu_1}+Ke^{-\mu_1 t}\tag{12}$$

At initial condition i.e. $t=0\Rightarrow N(t)=N(0)$. Then, the above equation becomes

$$\mathrm{N}(0)=\frac{b_p}{\mu_1}+K$$

or

$$\mathrm{N}(0) - \frac{b_p}{\mu_1} = K$$

Substituting K into Equation (12), we have

$$\mathrm{N}(t) = \frac{b_p}{\mu_1} + \left[N(0) - \frac{b_p}{\mu_1}\right] e^{-\mu_1 t} \geq 0,$$

where $N(0)$ is the initial population at time $t = t_0 = 0$. This result to the fact that $N(t) \leq N(0)$ as $t \to 0$ and $N(0) \leq 0$ as $t \to \infty$.

Inductively, using Birkhof and Rota's theorem of differential inequality [26], then when $t \to \infty$ we see that

$$0 \leq N(t) \leq \frac{b_n}{\mu_1}, \forall\, t \geq 0$$

Now, from system (2), we know that

$$\frac{dX_p}{dt} = \frac{dY}{dt} = \frac{dL}{dt} = \frac{dI}{dt} = \frac{dC}{dt} = \frac{dR}{dt} = 0$$

which implies that

$$\frac{dN}{dt} = 0$$

By integrating

$$\mathrm{N} = C$$

But

$$\mathrm{N} = X_p + Y + L + I + C + R = 1$$

Since population under investigation is unity. It follows that $C = 1$, implying that the population under study is constant, positive and is unity. Hence, $\mathfrak{R}_D = \left\{(X_p, Y, I, L, C, R) \in \mathfrak{R}_+^6 : X_p + Y + I + L + C + R = 1\right\}$. Thus, the model is attracting, bounded, and mathematically well posed. □

3.3. Existence and uniqueness of system solution

Theorem 3. *(Existence and uniqueness). The system (2) is continuous and satisfies Cauchy-Lipschitz condition.*

Proof. We explore existence and uniqueness results [27,28]. Then, we show from system (2), taking the first equation, while the rest follow similar procedures.

Now let.

$$Z(t,s) = \frac{dX_p}{dt} = b_p\omega(1 - vC) - \lambda X_p + (1 - \sigma)Y - (\sigma + \mu_1)X_p \tag{13}$$

Then, substituting mass action equation $\lambda = \frac{\beta(1-\eta C)}{N}$, into Equation (13), we obtain the partial derivatives as:

$$\frac{\partial Z(t,s)}{\partial s} = -\frac{\beta(1 - \eta C)}{N} - (\sigma + \mu_1) \tag{14}$$

This shows that the function $Z(t,s)$ and its partial derivatives $\frac{\partial Z(t,s)}{\partial s}$ are defined and continuous at all points (t,s). Similarly, the right-hand functions of other equations and their respective partial derivatives inductively satisfy these conditions. This imply that by existence and uniqueness theorem, there exists a unique solution for $X_p(t), Y(t), L(t), I(t), C(t), R(t)$ in some open intervals centered t_0. We then have to show that the solution satisfies the Lipschitz condition. Now using (13) we see at once that

$$\left|Z\left(t, s_{X_p(1)}\right) - Z\left(t, s_{X_p(2)}\right)\right| = \begin{vmatrix} \mu\omega(1-vC) - \left(-\frac{\beta(1-\eta C)}{N}\right) X_{p_{(1)}} - \sigma X_{p(1)} + (1-vC)Y - \mu_1 X_{p(1)} \\ -\mu\omega(1-vC) - \left(-\frac{\beta(1-\eta C)}{N}\right) X_{p_{(2)}} - \sigma X_{p(2)} + (1-vC)Y - \mu_1 X_{p(2)} \end{vmatrix}$$

$$= \left|(-)\left[\frac{\beta(1-\eta C)}{N} + \sigma + r + \mu_1\right]\left(X_{p(1)} - X_{p(2)}\right)\right|$$

$$\leq \left[\frac{\beta(1-\eta C)}{N} + \sigma + r + \mu_1\right]\left|X_{p(1)} - X_{p(2)}\right|$$

This implies that $\left|Z\left(t, s_{Xp(1)}\right) - Z\left(t, s_{Xp(2)}\right)\right| \leq M\left|X_{p(1)} - X_{p(2)}\right|$, where $M = \left(\frac{\beta(1-\eta C)}{N} + \sigma + r + \mu_1\right)$ is a Lipschitz constant. In a similar procedure, we show that the remaining variables satisfies the Lipschitz condition. Therefore, there exists a unique solution $X_p(t), Y(t), L(t), I(t), C(t), R(t)$ for all $t \geq 0$.□

4. Numerical computations

Table 3. Value specification for state and parameter variables of **Tables 1 and 2**

State-space		**Parameter variables**			
Symbols	**Values**	**Symbols**	**values**	**Symbols**	**Values**
X_p	0.4	b_p	0.0247	β_1	0.1
Y	0.1	ω	0.5	β_2	0.1
L	0.1	$(1-\omega)$	0.5	β_3	0.5
I	0.1	σ	0,65	β_4	0.95
C	0.1	$(1-\sigma)$	0.25	t_1	0.0525
R	0.1	μ_1	0.00693	$(1-\xi)$	0.67
		μ_2	0.31	ψ_e	0.297
		λ	$\in$ [0.1]	v	0.35
		β	0.98	ω_1	0.045
		η	0.45	ω_2	0.0.4
		ε_1	6/365	ω_3	0.6
		ε_2	8/365	ω_4	0.6
		ε_3	4/365	r	0.4

Note: **Table 3**, represent modified value generateds from motivating model [1].

Following the derivation of system model, generated numerical values are induced to **Tables 1** and **2**, to give us the required **Table 3**, desired of the present

numerical computations. Basically, we conduct two major simulations: the off-treatment scenario and at on-set application of control functions. The entire computations explored in-built Runge-Kutter of order of precision 4, in a Mathcad surface. The empirical **Table 3**, is as seen below:

4.1. Numerical simulation of system model under off-treatment ($\omega = 0, \sigma = 0, \nu = 0, t_1 = 0$)

Of note, derived model represents a set of 6-dimensional nonlinear ordinary differential equation involving 6 sub-populations. Using **Table 3**, the basic model equation is simulated for off-treatment scenario as depicted by **Figure 2a**–**f**.

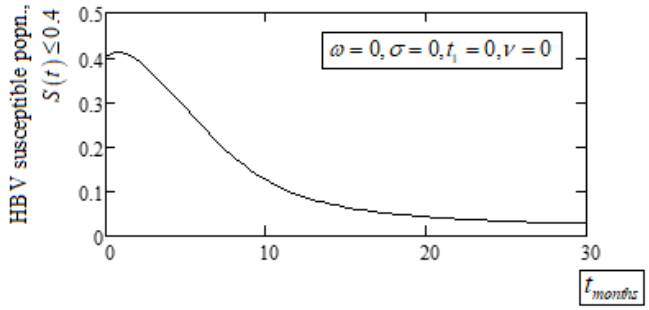

(a) HBV susceptible popn. under off-treatment, $\mu = 0.045$.

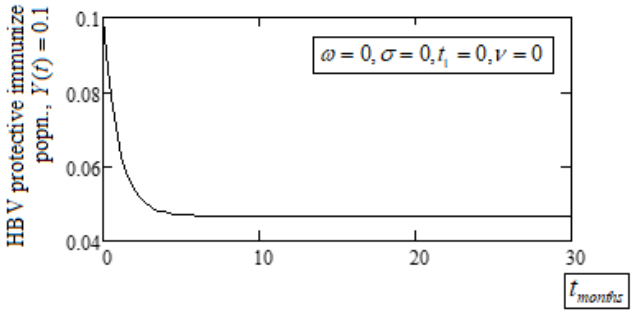

(b) HBV protective immunize popn. under off-treatment, $\beta = 0.98$.

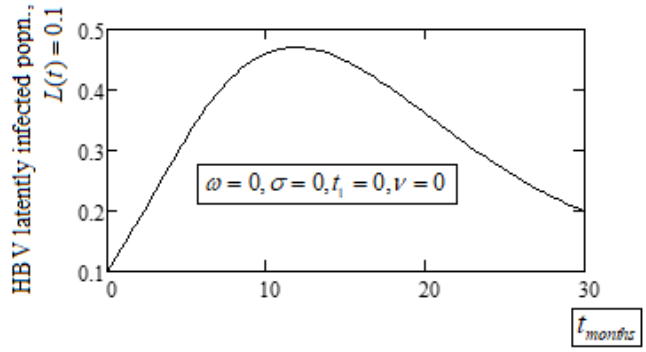

(c) HBV latently infected popn. under off-treatment, $\beta = 0.98$.

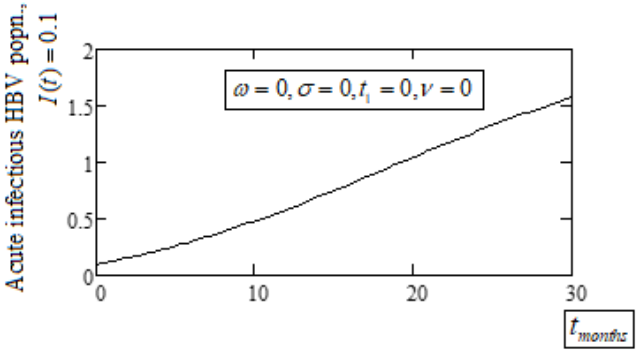

(d) Acute infectious HBV popn. under off-treatment, $\beta = 0.98$.

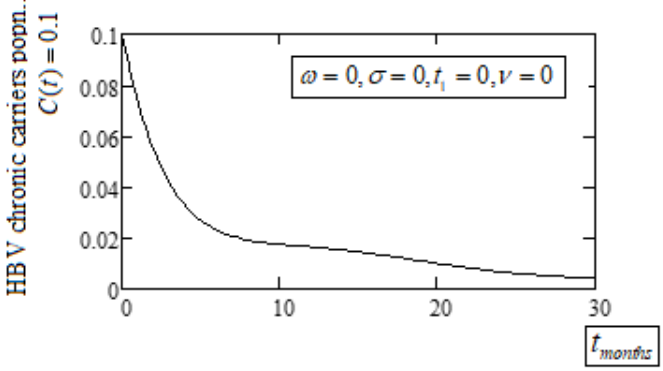

(e) HBV chronic carriers popn. under off-treatment, $\beta = 0.98$.

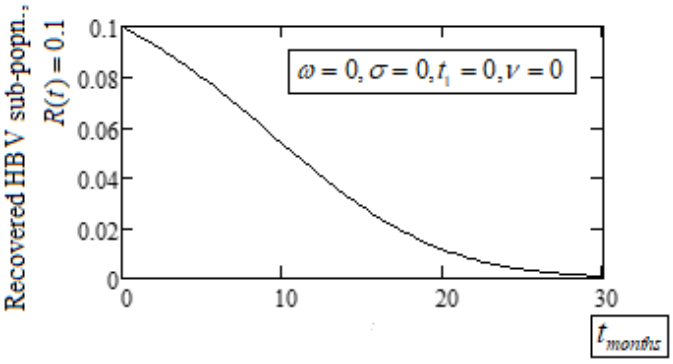

(f) HBV recovered sub-popn. under off-treatment, $\beta = 0.98$.

Figure 2. Dynamic flow of infectious HBV model under off-treatment scenario, $\mu = 0.47$, $\beta = 0.98$.

From **Figure 2a**, the simulation depicts a class of HBV susceptible population investigated under off-treatment scenario. This compartment exhibits steady decline with value range of $0.028 \leq X(t) \leq 0.4$ for all $t_f \leq 30$ months. Under the protective immunized sub-population $Y(t)$, as depicted by **Figure 2b**, rapid decline is observed following non-inducement of immunization control functions with declining value range of $0.047 \leq Y(t) \leq 0.1$ for all $t_f \leq 30$ months. **Figure 2c** represent the latently HBV infected sub-population under off-treatment scenario. This compartment exhibit initial inclination with value range of $0.1 \leq L(t) \leq 0.47$ at $t_f \leq 12$ month. Thereafter, the curve exhibited concave declination due to lack of control functions with decline value of $L(t) \leq 0.2$ for all $12 \leq t_f \leq 30$ months.

From **Figure 2d**, the simulation observed a smooth inclined rate of acute infected HBV sub-population under off-treatment scenario. This depicts high spread of the virus under no control functions $0.1 \leq I(t) \leq 1.572$for all $t_f \leq 30$ months. **Figure 2e** represent chronic carriers of HBV infection under off-treatment. The study observe that in the absence of any control function, there exist a rapid extinction infections HBV in this deteriorating value of $0.1 \geq C(t) \geq 4.212 \times 10^{-3}$ for all $t_f \leq 30$ months. Furthermore, the compartment for recovered population depicted by **Figure 2f** initiate smooth rapid linear decline to near zero due to complete lack of any control function $0.1 \geq R(t) \geq 8.147 \times 10^{-4}$ for all $t_f \leq 30$ months.

4.2. Numerical simulation of system model under onset-treatment, $(\omega, \sigma, v, t_1) \geq 0$

Furthermore, the investigation consider derived model with the introduction of control functions denoted by (ω, σ, v, t_1)**,** while other parameters remains the same as in Section 4.1. Thus, the required simulations involving the 6 subpopulations are depicted by **Figure 3a**–**f** below:

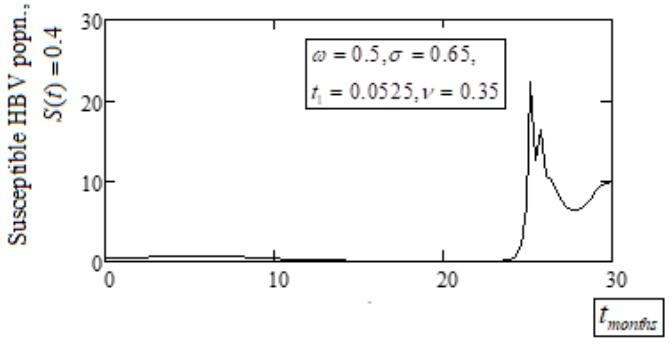

(a) HBV susceptible popn. under onset-treatment, $\mu = 0.045$.

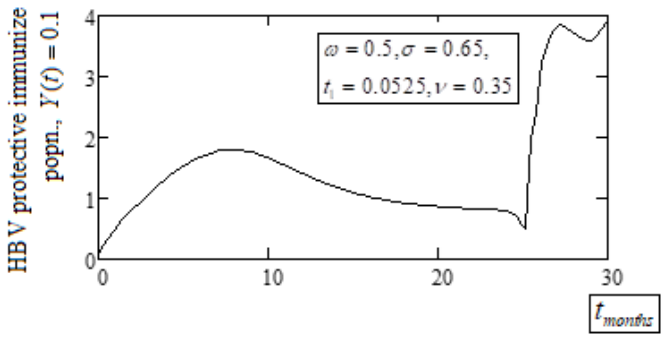

(b) HBV protective immunize popn. under onset-treatment, $\beta = 0.98$.

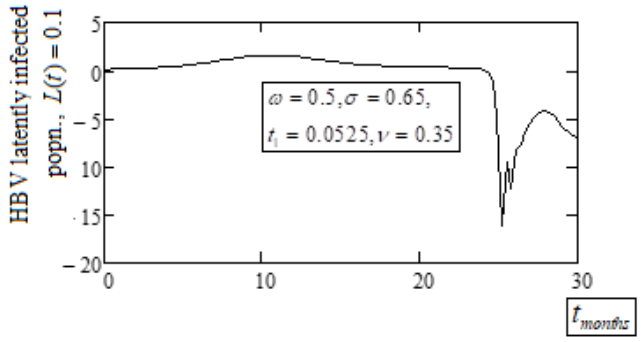

(c) HBV latently infected popn. under onset-treatment, $\beta = 0.98$.

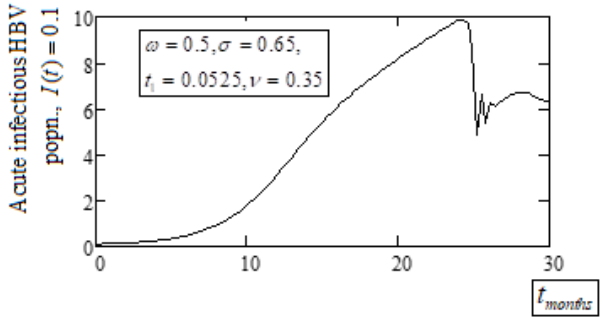

(d) HBV acute infectious popn. under onset-treatment, $\beta = 0.98$.

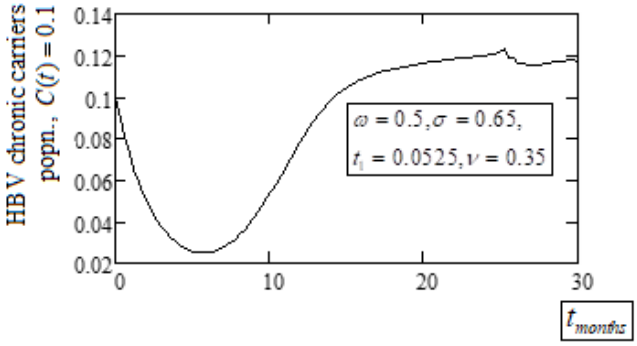

(e) HBV chronic carriers popn. under onset-treatment, $\beta = 0.98$.

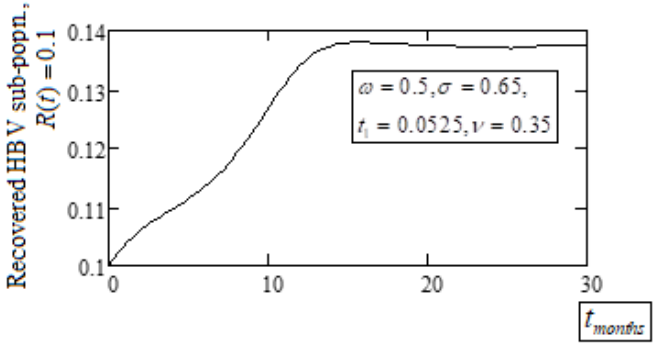

(f) HBV recovered sub-popn. under onset-treatment, $\beta = 0.98$.

Figure 3. Dynamic flow of infectious HBV model under onset-control functions, $\mu = 0.47, \beta = 0.98$.

Figure 3a represents the susceptible compartment under coherent treatment functions. It is observe that an initial declined population in the first 20 months is seen exhibiting rapid inclination, following the introduction of designated control functions with maximum value range of $0.051 \leq X_p(t) \leq 22.322$ at $0 \leq t_f \leq 24$ month but declined We saw slightly for all $24 \leq t_f \leq 30$ months with value at $22.322 \leq X_p(t) \leq 10.088$. **Figure 3b** exhibits undulating inclined immunize sub-population due to induce control function with maximal value of $0.1 \leq Y(t) \leq 3.92$ at $t_f \leq 30$ months. In **Figure 3c**, the simulation describes the dynamic of latently infected sub-population under coherent application of control functions. It is observe that the curve exhibited initial stable latently infectious class is seen declining with minimum value range of $16.223 \times 10^{-1} \leq L(t) \leq 8.78 \times 10^{-1}$ for all $24 \leq t_f \leq 30$ months.

Figure 3d illustrate the presence of control functions in compartment of acute infected sub-population. The investigation observe initial inclined linear curve with $0.1 \leq I(t) \leq 9.864$ at $t_f \leq 24$ months. However, with the introduction of control functions, acute infected population is seen declining rapidly with minimal value of $I(t) \geq 5.82$ at $24 \leq t_f \leq 30$ months. Under coherent control function, chronic carrier displace an undulating concave declination as depicted by **Figure 3e**. Dynamic variation of compartment Centre is in the range of $0.1 \geq C(t) \geq 0.06$ at $t_f \leq 6$ months and $0.06 \leq C(t) \leq 0.124$ at $6 \leq t_f \leq 30$ months. The recovered population under coherent control function depicted by **Figure 3f**, is seen to exhibit a steady inclined

linear curve at $t_f \leq 12$ month. With value at $0.1 \leq R(t) \leq 0.138$. Thereafter, the compartment observed steady state for all $12 \leq t_f \leq 30$ months.

5. Analysis of results of numerical computations

So far in this investigation, a 6-Dimensional HBV mathematical dynamic model have been developed, following the extension and modification of system motivating model [1]. The derived model was investigated using bilinear control functions in conjunction with application of monolithic vaccination. System analytical predictions focuses on the mathematical and epidemiological well-posedness of derived HBV model. In conjunction with fundamental differential theory, the investigation explored classical Cauchy-Lipschitz condition for the establishment of existence and uniqueness of system solutions.

Numerical simulations were conducted with clear indications that under off-treatment scenario, both the susceptible and protective immunized compartments as well as the recovery chamber exhibited rapid population declined to near-zero outcome for all $t_f \leq 30$ months. This delineative output was evidenced by the surging inclination rate exhibited by latently, acute and chronic carriers' subpopulations. The introduction of bilinear control functions enhanced by induced monolytic vaccination saw rejuvenated of both the recovery compartment and the susceptible state-space as depicted by **Figure 3a**–**f**.

Furthermore, the present results were an improvement to those of system motivating model in spite of diverging set goals. For instance, the main component of simulations of system motivating model was its system reproduction numbers as against the current target of behavioral impact of designated control functions. Moreso, we observed from system motivating model that infection of HBV at protective compartment where $R_0 = 1$, was intensively high, which can be aligned to the case of non-vaccine and lack of control functions for the present investigation. None-the-less, the present investigation depicts simplified methodological application of designated control function with specified vaccine, leading to a more seeming optimal results.

6. Conclusion and recommendations

Remarkably, amid novel results from dynamic controls of HBV infection, the present investigation presented a simplified, dynamic, 6-dimensional mathematical model. The goal of the study was the methodological implementation of bilinear control functions in conjunction with designated monolytic vaccination. Moreover, the study dwells on the determination of system mathematical and epidemiological well-posedness as well as the behavioral impact of treated recovered populations on the susceptible population. In affirmation of aforementioned research goal, simulated results substantially indicated that under off-treatment scenario, population under HBV infectivity exhibited rapid extinction behavior for all $t_f \leq 30$ months.

Resourcefully, the application of designated control functions aligned with vaccination exhibited tremendous suppression of the viral load, leading to rejuvenation of the recovery and the susceptible subpopulations with diminished latently and

acutely infected subpopulations. The overall outcome extensively dignified the study set goal, as results can be used for decision control policies by health sectors and biosciences research advancement. Moreover, the method could be replicated for HBV-related co-infectivity. Notably, the adverse impact of therapy abuse was not accounted for by this study. A process, if incorporated into existing study, could lead to future investigation.

Acknowledgments: The author otherwise known as the correspondent inevitably expressed his deep appreciation to my anonymous reviewers whose scientific know-how have deepened the standard of the final output of this article.

Conflict of interest: The author declares no conflict of interest.

References

1. Jannatun N, Chandra NP. A Mathematical study on the vaccination impact on the disease dynamics of HBV. IOSR Journal of Mathematics (IOSR-JM). 2014; 10(6): 26–44.
2. Atteena PK, Bultery M, Hu DJ, Jamieson DJ. HIV-HBV co-infection–A global challenge. N. Engl J. Med. 2012; 366(19): 1749–1752.
3. Hagiwara S, Nishida N, Kudo M. Antiviral therapy for chronic hepatitis B: Combination of nucleoside analogs and interferon. World Journal of Hepatology. 2015; 7(23): 2427–2431.
4. Nasal M. HBV cccDNA: Viral persistence reservoir and key obstacle for a cure of chronic hepatitis B. Gut. 2015; 64: 1972–1984.
5. AHweiss L, Dandri M. A Review: The Role of cccDNA in HBV Maintenance. Available online: https://www.ncbi.nlm.nih.gov/pmc/articles/PMC5490831/pdf/viruses-09-00156.pdf (accessed on 27 July 2024).
6. World Health Organization. Key fact on Hepatitis B. Available online: https://www.who.int/news-room/fact-sheets/detail/hepatitis-b (accessed on 27 July 2024).
7. Alavian SM. Hepatitis B virus infection in Iran: Changing the epidemiology. Iran J clin infect Dis.2010; 5: 51–61.
8. Bassey EB. Dynamic optimal control model for dual-pair treatment functions of dual delayed HIV-pathogen infections. Journal of Mathematical Sciences: Advances and Applications. 2018; 51(1): 1–50.
9. Culshaw R, Ruan S, Spiteri RJ. Optimal HIV Treatment by Maximizing Immune Response. Journal of Mathematical Biology. 2004; 48(5): 545–562.
10. Allali K, Meskaf A, Tridane A. Mathematical modeling of the adaptive immune responses in the early stage of the HBV infection. International Journal of Differential Equations. 2018; 1: 1–13.
11. Webster GJM, Reignat S, Miani MK, et al. Incubation phase of acute hepatitis B in man: Dynamics of cellular immune mechanisms. Hepatology. 2000; 32(5): 1117–1124.
12. Bassey BE. Optimal Control Dynamics: Multi-therapies with Dual Immune Response for Treatment of Dual Delayed HIV-HBV Infections. International Journal of Mathematical Sciences and Computing (IJMSC). 2020; 6(2): 18–60.
13. Manna K, Chakrabarty SP. Combination therapy of pegylated interferon and lamivudine and optimal controls for chronic hepatitis B infection. Int. J. Dynam. Control. 2018; 354–368.
14. Yousfi N, Hattaf K, Tridane A. Modeling the adaptive immune response in HBV infection. J. Math. Biol. 2011; 63: 933–957.
15. Dontwi IK, Frempong NK, Wiah EN. Using mathematical model to depict the immune response to Hepatitis B virus infection. American Journal of Sc. & Ind. Res. 2010; 1(3): 516–528.
16. Medley GF, Lindop NA, Edmunds WJ, Nokes DJ. Hepatitis-B virus endemicity: heterogeneity, catastrophic dynamics and control. Nat Med. 2001; 7(5): 619–624.
17. Zou L, Zhang W, Ruan S. Modeling the transmission dynamics and control of hepatitis B virus in China; Journal of Theoretical Biology. 2010; 262: 330–338.
18. Mandell GL, Douglas RG, Bennett JE. Principles and Practice of infectious Diseases. A Wiley Medical Publication John Wiley and Sons; 1979.

19. Shepard CW, Simard EP, Finelli L, et al. Hepatitis B virus infection: epidemiology and vaccination. Epidemiologic Reviews. 2006; 28: 112–125.
20. Eikenberry S, Hews S, Nagy JD, Kuang Y. The dynamics of a delay model of hepatitis B virus infection with logistic hepatocyte growth. Mathematical. Biosciences and Engineering. 2009; 6(2): 283–299.
21. Nancy FC, Mark RW. Vaccination in HIV-infected Adults. Clinical and Epidemiologic Research. 2014; 28(8): 397–410.
22. Akanni JO, Akinpelu FO. Sensitivity analysis of HIV/AIDS model with vertical transmission, treatment and progression rate. International Journal of Scientific and Engineering Research. 2016; 7(8): 497–514.
23. Edward S, Nyerere N. A Mathematical Model for the Dynamics of Cholera with Control Measures. Applied and Computational Mathematics. 2015; 4(2): 53–63.
24. Bassey EB, Adagba OH. Global stability analysis of the role of antiretroviral therapy (ART) abuse in HIV/AIDS treatment dynamics. Pure and Applied Mathematics Journal. 2021; 10(1): 9–31.
25. Osman S, Makinde OD, Theuri DM. Stability analysis and modeling of listeriosis dynamics in human and animal populations. Global Journal of Pure and Applied Mathematics. 2018; 14(1): 115–138.
26. Mafuta P, Mushanyu J, Nhawu G. Invariant Region, Endemic Equilibria and Stability Analysis. IOSR Journal of Mathematics. 2014; 10(2): 118–120.
27. Ezegu NJ, Togbenon HA, Moyo E. Modeling and Analysis of Cholera Dynamics with Vaccination. American Journal of Applied Mathematics and Statistics. 2019; 7: 1–8.
28. Bassey EB, Igwe OE. On Determinism, Well Posedness and the Application of Cauchy-Lipchitz conditions for a hypo-Hypercovid-19 Epidemic Model. Unicross Journal of Science and Technology. 2022; l1(2): 91–108.